JOURNAL OF APPLIED PHYSICS **113**, 024508 (2013)

Major and minor stress-magnetization loops in textured polycrystalline $Fe_{81.6}Ga_{18.4}$ Galfenol

Ling Weng,[1,2] Travis Walker,[2] Zhangxian Deng,[2] M. J. Dapino,[2,a)] and Bowen Wang[1]
[1]*Key Laboratory of Electro-Magnetic Field and Electrical Apparatus Reliability of Hebei Province, Hebei University of Technology, Tianjin 300130, China*
[2]*Department of Mechanical and Aerospace Engineering, The Ohio State University, Columbus, Ohio 43210, USA*

(Received 25 July 2012; accepted 4 December 2012; published online 10 January 2013)

Major and minor magnetization versus stress loops under different bias magnetic fields from 0.8 kA/m to 8.0 kA/m in 0.8 kA/m steps were measured in research grade, ⟨100⟩ oriented, textured polycrystalline $Fe_{81.6}Ga_{18.4}$. Both compressive and tensile stresses were applied from −63 MPa to 63 MPa for major loop analysis. Minor loops were generated by superimposing a 4.0 Hz, 2.8 MPa amplitude sinusoidal stress on different dc compressive stresses ranging from −40.7 MPa to −5.6 MPa in 7.0 MPa increments. Bias magnetic fields were applied in two ways, constant field in the sample obtained using a controller and constant current to the excitation coils. An energy-averaged model and related optimization method are presented to compare the experiments with simulations. The slope of magnetic flux density versus stress, i.e., the material's sensitivity to stress, is quantified from major and minor loop measurements. The peak sensitivity at constant field is about 75 T/GPa for constant-field major loops, whereas it is 41 T/GPa for constant-current major loops. The sensitivity for minor loops is consistently lower than for major loops, whether at constant field or constant current. © *2013 American Institute of Physics*. [http://dx.doi.org/10.1063/1.4772722]

I. INTRODUCTION

Magnetostrictive materials deform when exposed to magnetic fields and change their magnetization when mechanically stressed. These behaviors can be used to design actuators and sensors. Iron-gallium alloys (Galfenol), an emerging class of magnetostrictive materials, exhibit moderate magnetostriction ($\sim 350 \times 10^{-6}$) at low magnetic fields ($\sim$8 kA/m) along with low magnetic hysteresis and high tensile strength.[1] These unique properties make Galfenol better suited in certain actuation and sensing applications than piezoelectric materials and Terfenol-D. The sensing effect, magnetization change in response to stress, is the enabling principle for magnetoelastic sensors.[2]

Major loop magnetization compressive tests, consisting of loading from zero load to −110 MPa and subsequent unloading, at magnetic fields ranging from 0 to 71.28 kA/m (891 Oe) were performed on single-crystal 19% and 24% Ga samples.[3,4] An energy-based model was employed by Atulasimha *et al.*[5,6] to describe actuation and sensing behavior at various bias fields for single-crystal Fe-Ga alloys. Major magnetization versus stress loops under constant magnetic field ranging from 0 to 71.2 kA/m were measured and modeled on ⟨100⟩ oriented single-crystal Fe-Ga alloys subjected to compressive stresses ranging from −120 MPa to 0 MPa.[7,8] A magnetic hysteresis model for field and stress application in Galfenol has been presented by Evans and Dapino.[9–11] Unlike prior energy-averaged models that rely on a large number of moment orientations, this model considers only 6 fixed orientations which correspond with Galfenol's easy crystallographic axes. An important benefit of the reduced order is that the model runs 100 times faster than previous energy-weighting models while also being accurate for materials with any magnetocrystalline anisotropy. Magnetic moment switching occurs immediately once the energy difference between orientations exceeds a certain threshold. Weetman and Akhras[12] added a rate term taking the transition time into consideration, making the model rate-dependent. The model is satisfactory at low bias fields but its accuracy diminishes substantially for higher bias fields. It is suggested that more than one fitting parameter is needed for improved accuracy to be achieved at high bias fields.

A polycrystalline material is attractive for applications due to its reduced cost relative to single-crystal material. Major magnetization versus stress loops of production grade polycrystalline $Fe_{81.6}Ga_{18.4}$ have been measured over the range from −120 MPa to 0 MPa and bias fields from 0 to 71.28 kA/m (891 Oe).[13] The experiments and energy-based model simulation do not correlate well for the higher bias magnetic fields tested. Even for compressive stresses as high as 110 MPa, the high bias fields prevent the rotation into the transverse direction. The effect of stress on magnetic susceptibility and applications to force sensing in textured polycrystalline $Fe_{81.6}Ga_{18.4}$ and $Fe_{79.1}Ga_{20.9}$ have also been investigated.[14,15] The results show that the susceptibility change of $Fe_{81.6}Ga_{18.4}$ at stresses ranging from −10 to 20 MPa is linear and larger than it is for $Fe_{79.1}Ga_{20.9}$, indicating that $Fe_{81.6}Ga_{18.4}$ is preferable for force sensing in this stress range. Measurements of the linear piezomagnetic coefficients d_{33}^{*}, d_{33}, and d_{33}^{ϕ} were made on $Fe_{81.6}Ga_{18.4}$ textured polycrystalline rods for energy harvesting applications.[16] Here, the bias field was not held constant because energy harvesting devices typically do not require bias field control.

a)Author to whom correspondence should be addressed. Electronic mail: dapino.1@osu.edu.

Different stress differentials between ±25 MPa and ±0.5 MPa at 8.0 kA/m (100 Oe) and one dc compressive stress which was in the center of the active region were tested. It was shown that the peak d_{33}^{ϕ} values are lower than the d_{33}^{*} values: The largest d_{33}^{*} was 60 nm/A for a bias field of 8.0 kA/m and dc compressive stress of −33 MPa, while d_{33}^{ϕ} was 30 nm/A at the same bias field and stress.

Stress or force sensors based on Galfenol are attractive due to their contact-less signal collection, ruggedness, and ease of integration facilitated by Galfenol's structural properties. Such sensors must reliably operate for both minor and major loop stress inputs. Characterization of minor magnetization versus stress loops under different bias fields and different dc compressive stresses has been lacking. Major magnetization versus stress loops in tension and low compressive stresses that are suitable for sensors also must be studied. In this work, major loop magnetization measurements of research grade, ⟨100⟩ oriented, textured polycrystalline $Fe_{81.6}Ga_{18.4}$ were conducted in compression and tension ranging from −63 MPa to 63 MPa at a frequency of 0.05 Hz and different bias fields. The focus on 18.4 at. % alloys is motivated by the previous literature, in particular the linear susceptibility demonstrated by Mahadevan *et al.*[14] over the range from −10 to 20 MPa. Single-crystal Galfenol alloys have maximum sensitivity when the bias magnetic field is below 5 kA/m;[7] therefore, magnetic fields in this work were applied from 0 to 8.0 kA/m in 0.8 kA/m steps. The magnetic field was applied in two ways: constant field in the sample using a controller and constant current to the excitation coils. Minor magnetization loops under different bias fields were tested on the same material. The dc compressive stresses were varied from −40.7 MPa to −5.6 MPa in 7.0 MPa steps while superimposing a 4 Hz, 2.8 MPa amplitude sinusoidal stress. The Evans and Dapino energy-averaged model[9–11] was used to describe the experimental data. The results show close agreement with an error of 1.18% for constant field and 1.38% for constant current.

II. MAJOR AND MINOR LOOP MEASUREMENTS

The polycrystalline $Fe_{81.6}Ga_{18.4}$ Galfenol sample used in this study has a diameter of 6.35 mm (0.25 in.) and a length of 73.66 mm (2.9 in.). The sample was placed in the middle of a transducer which consists of the Galfenol rod, laminated steel sheets, excitation coils, and a pick-up coil (Fig. 1).[17] The cyclic stress was applied using a Test Resources R Series Controller load frame. The magnetic flux density was measured using a Walker Scientific MF 5D fluxmeter and a pick-up coil located midway along the length of the Galfenol rod. The bias magnetic fields were measured using an Allegro A1322LUA-T Hall chip, and were applied in two ways: using a dSpace 1104 system programmed for proportional-integral (PI) control to keep the magnetic field in the sample constant throughout the stress cycle and applying a constant current to the excitation coils. The controller eliminates the interaction between the sample and the magnetic circuit. A LabVIEW system was used to record the data. The magnetization was calculated by subtracting the applied field from the flux density measurements.

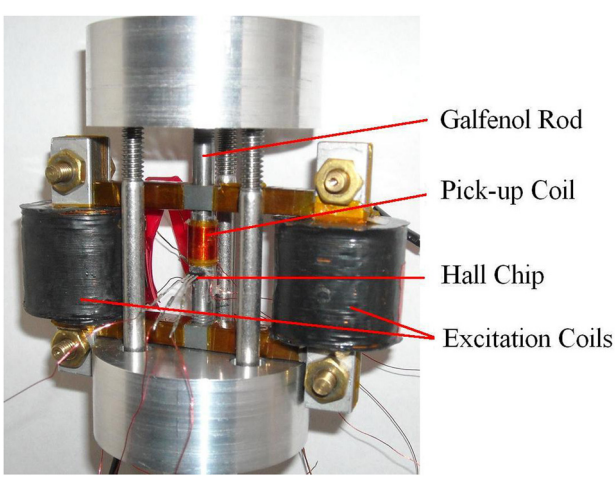

FIG. 1. Galfenol device employed for characterization of major and minor magnetization loops.

The major magnetization versus stress loop testing procedure included application of a bias field at zero load followed by application of 0.05 Hz cyclic stresses. The biasing procedure consisted of bringing the Galfenol sample to saturation with a 1.0 A current to the coils and then decreasing the current until the desired bias field was reached. Magnetic biasing for the minor loop tests was performed in the same manner. Subsequently, a dc compressive stress was applied by the Test Resources machine at a constant rate of 1.05 MPa/s. A 4.0 Hz, 2.8 MPa amplitude sinusoidal stress was then applied with the Test Resources machine in feedback load control mode. At a given bias field, the mechanical loading was repeated for different dc compressive stresses ranging from −40.7 MPa to −5.6 MPa in 7.0 MPa steps.

III. ENERGY-AVERAGED MODEL AND OPTIMIZATION

The free energy of a magnetostrictive material has terms for magnetic anisotropy, magnetomechanical coupling, and Zeeman (magnetic field) energy. Evans and Dapino[9] developed a coupled, energy-averaged constitutive model for magnetostrictive materials by choosing orientations which minimize an energy function locally defined in the vicinity of each easy axis. The total free energy of each particle variant (denoted k) is[9]

$$G^k = \frac{1}{2}K^k|\mathbf{m}^k - \mathbf{c}^k|^2 - \mathbf{S}_m^k \cdot \mathbf{T} - \mu_0 M_s \mathbf{m}^k \cdot \mathbf{H}, \qquad (1)$$

where $G_A^k = \frac{1}{2}K^k|\mathbf{m}^k - \mathbf{c}^k|^2$ is the anisotropy energy associated with rotating a Stoner-Wohlfarth (SW) particle away from the easy direction $\mathbf{c}^k$. The term $G_C^k = \mathbf{S}_m^k \cdot \mathbf{T}$ is the magnetomechanical coupling energy whereas $G_Z^k = \mu_0 M_s \mathbf{m}^k \cdot \mathbf{H}$ is the Zeeman energy. For describing the anisotropy energy of stress-annealing, which induces tetragonal anisotropy in Galfenol, Chakrabarti and Dapino[18] added a constant term K_0^k as follows:

$$G^k = \frac{1}{2}K|\mathbf{m}^k - \mathbf{c}^k|^2 + K_0^k - \mathbf{S}_m^k \cdot \mathbf{T} - \mu_0 M_s \mathbf{m}^k \cdot \mathbf{H}. \qquad (2)$$

In matrix form, definition (2) can be expressed as[18]

$$G^k = \frac{1}{2}\mathbf{m}^k \cdot \mathbf{K}\mathbf{m}^k - \mathbf{m}^k \cdot \mathbf{B}^k + \frac{1}{2}K + K_0^k, \tag{3}$$

where the magnetic stiffness matrix $\mathbf{K}$ and force vector $\mathbf{B}^k$ are

$$\mathbf{K} = \begin{bmatrix} K - 3\lambda_{100}T_1 & -3\lambda_{111}T_4 & -3\lambda_{111}T_6 \\ -3\lambda_{111}T_4 & K - 3\lambda_{100}T_2 & -3\lambda_{111}T_5 \\ -3\lambda_{111}T_6 & -3\lambda_{111}T_5 & K - 3\lambda_{100}T_3 \end{bmatrix}, \tag{4}$$

$$\mathbf{B}^k = [\, c_1^k K + \mu_0 M_s H_1 \quad c_2^k K + \mu_0 M_s H_2 \quad c_3^k K + \mu_0 M_s H_3 \,]^T. \tag{5}$$

The magnetic orientations $\mathbf{m}^k$ of SW particles are calculated from minimization of the free energy with constraint $\mathbf{m}^k \cdot \mathbf{m}^k = 1 \approx \mathbf{c}^k \cdot \mathbf{m}^k = 1$, which gives

$$\mathbf{m}^k = (\mathbf{K})^{-1}\left[\mathbf{B}^k + \frac{1 - \mathbf{c}^k \cdot (\mathbf{K})^{-1} \cdot \mathbf{B}^k}{\mathbf{c}^k \cdot (\mathbf{K})^{-1} \cdot \mathbf{c}^k} \cdot \mathbf{c}^k\right]. \tag{6}$$

The anhysteretic values of the volume fractions are calculated using Boltzmann-type averaging[9,18]

$$\xi_{an}^k = \frac{\exp(-G^k/\Omega)}{\sum_{k=1}^{r} \exp(-G^k/\Omega)}, \tag{7}$$

in which Ω is a smoothing factor.[19] The anhysteretic magnetization $\mathbf{M}$ is the sum of the magnetization $M_s\mathbf{m}^k$ due to each orientation, weighted by the volume fraction ξ_{an}^k of particles in each orientation[9]

$$\mathbf{M} = M_s \sum_{k=1}^{r} \xi_{an}^k \mathbf{m}^k. \tag{8}$$

There are six parameters in this model: anisotropy constants K and K_0, smoothing factor Ω, magnetostriction constants λ_{100} and λ_{111}, and saturation magnetization M_s. Because of the cubic symmetric crystal structure of Galfenol, the anisotropy constants along the 6 orientations are the same and equal to K. According to (3), an incremental value K_0 is used to modify the anisotropy constants along the directions [100] and $[\bar{1}00]$ in which the stress and field are applied. Chakrabarti and Dapino[18] developed a two-step parameter estimation method from one-dimensional (1D) measurements. First, the anhysteretic curves from hysteretic measurements are obtained through a simple averaging procedure. Next, a least squares optimization routine is used to minimize the error between the family of modeled curves and the anhysteretic curves obtained from measurements. The optimized parameters from 1D measurements can be used directly in three-dimensional (3D) finite element analysis for Galfenol systems instead of performing 3D measurements.

IV. RESULTS AND DISCUSSION

A. Major magnetization loops under constant field

Fig. 2(a) shows constant-field magnetization versus stress measurements at different bias fields. The stress was cycled from 63 MPa (tension) to −63 MPa (compression) and back to 63 MPa at a frequency of 0.05 Hz. The bias magnetic fields range from 0.8 kA/m to 8.0 kA/m in 0.8 kA/m steps. The energy-averaged model presented in Sec. III was utilized to describe the measurements as shown in Fig. 2(b). Since the model is anhysteretic, an averaging technique[18] was used to extract anhysteretic curves from the measured data. There is extremely close agreement between the model and experiments, with an average error of 1.18%. For the optimization process, the constant λ_{111} is ignored: the stress and magnetic field are applied along the $\langle 100 \rangle$ direction and λ_{111} does not participate in the calculations. The optimizated parameters are $K = 27.1\,\mathrm{kJ/m^3}$, $K_0 = 0.021\,\mathrm{kJ/m^3}$, $\mu_0 M_s = 1.3787\,\mathrm{T}$, $\lambda_{100} = 156.56 \times 10^{-6}$, and $\Omega = 776.73\,\mathrm{J/m^3}$. The value for $\mu_o M_s$ is lower than the typical saturation induction for Galfenol with 18%-19% Ga. Generally, the magnetization for polycrystalline Galfenol is a bit lower than that of single-crystal Galfenol. Our measurements were cross-checked by plotting stress-magnetization data points on top of field-magnetization curves. These measurements match as shown in Fig. 3.

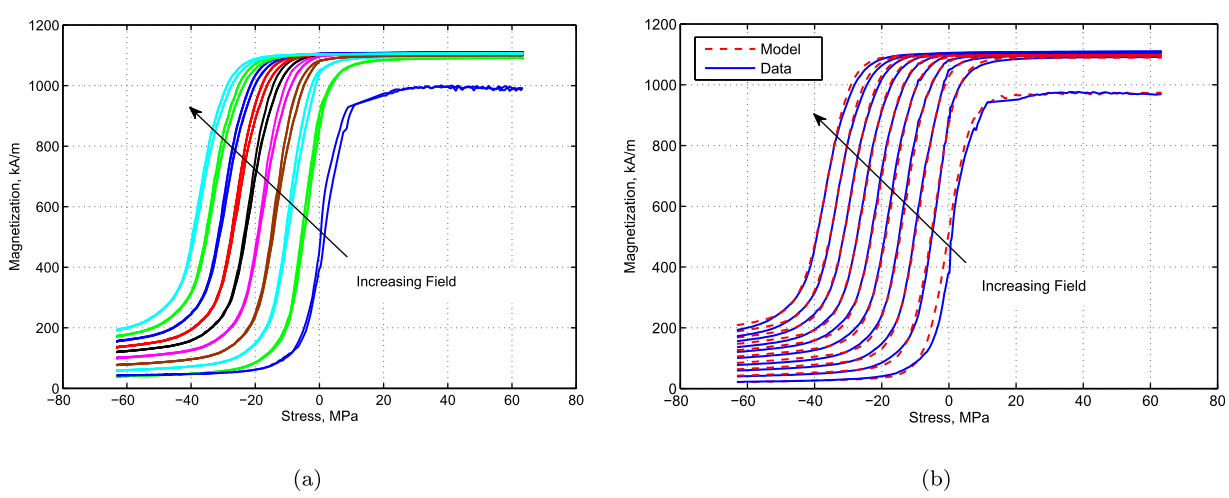

FIG. 2. (a) Constant-field magnetization versus stress measurements for bias magnetic fields of 0.8, 1.6, 2.4, 3.2, 4.0, 4.8, 5.6, 6.4, 7.2, and 8.0 kA/m. (b) Energy-averaged model results and averaged (anhysteretic) measurements.

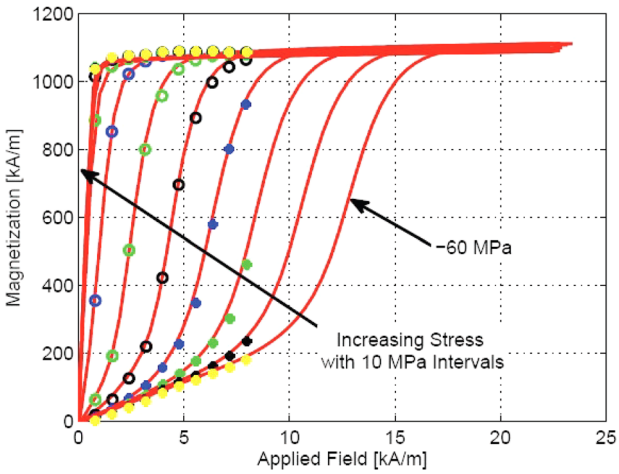

FIG. 3. Anhysteretic averages for magnetization versus field curves (red lines) and magnetization versus stress data points (dots).

In Fig. 2(a), the magnetization in the burst region varies steeply as a function of stress for the various bias magnetic fields. The bias field was applied along the length of the sample, and it causes the domains to align along the ⟨100⟩ direction. Compressive stress causes the domains to rotate perpendicular to the direction of the applied stress and magnetic field. It is seen in Fig. 2(a) that when the bias field is low, it is not sufficient to align all domains along ⟨100⟩. This means that an increasing bias field causes increasing magnetization under the same stress and displacement of the burst region where volume fraction changes occur. When the bias field is higher than 2.4 kA/m, the tensile stress has little or no effect on the magnetization because all the domains have aligned along the ⟨100⟩ direction and the material is saturated. For a bias field of 8.0 kA/m, there is full moment alignment along ⟨100⟩ and the magnetization does not change under tension. However, tensile stresses affect the magnetization considerably when bias fields are lower than 2.4 kA/m. When tension is applied at 0.8 kA/m, for instance, the magnetization changes from 380 kA/m to 980 kA/m.

In Fig. 2(a), there are two saturation regions: (1) magnetic field induced saturation when magnetic fields are high and stresses are low, and (2) stress induced saturation when magnetic fields are low and stresses are high. In the former case, the magnetic field energy dominates the total free energy, which causes alignment of domains along the ⟨100⟩ direction to balance magnetic energy and mechanical energy.

In the latter case, however, magnetomechanical coupling energy dominates the total free energy, which causes domains to rotate into directions perpendicular to ⟨100⟩. The field induced magnetization reaches a maximum value which corresponds to the situation in which all the domains are aligned along ⟨100⟩. Hysteresis is significant in the burst region which is explained by Evans and Dapino[9] as the Zeeman energy is generally larger than the magnetomechanical coupling energy.

The sensitivity (slope of magnetic flux density versus stress) versus stress at constant field shown in Fig. 4(a) was calculated from data in which the stress was decreased from tension to compression. The calculation method is a moving average scheme to reduce the large error that can arise if numerical differentiation is performed on experimental data.[8] A window of 130 points was chosen and a straight line was fitted to all 92 000 data points. As seen in the plot, the sensitivity for each applied magnetic field is stress-dependent. The peak sensitivity moves progressively toward increasing compression as the bias field is increased. The point at which the peak occurs is when the applied compressive stress balances the anisotropy energy and the magnetic field energy; small changes in stress around this point would result in large changes in magnetization which is most desired for sensors.[7,8] The maximum sensitivity is about 75.5 T/GPa, and occurs at low bias field and low compressive stress, 1.6 kA/m and −3.6 MPa, respectively.

When the stress increases from compression to tension, the sensitivity shows a different curve from that when stress is decreased from tension to compression. For clarity, this is illustrated in Fig. 4(b) by plotting curves at 1.6, 4.0, and 8.0 kA/m. The solid lines indicate a decreasing stress from 60 MPa to −60 MPa, while the dashed lines indicate an increasing stress from −60 MPa to 60 MPa. There is a reversal of maxima between the solid and dashed lines: at 1.6 kA/m,

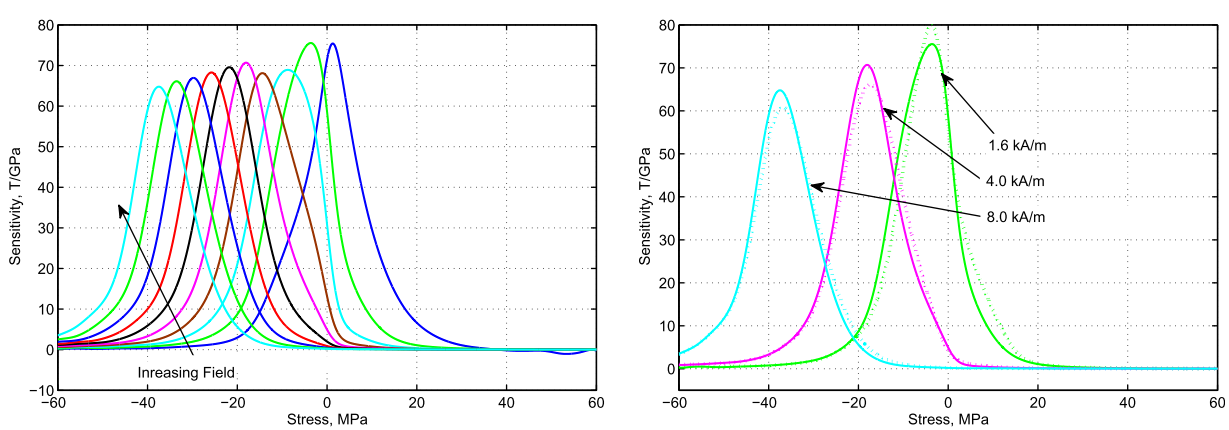

FIG. 4. (a) Sensitivity versus stress for constant field measurements (stress is decreased from 60 MPa to −60 MPa). (b) Sensitivity versus stress for bias fields of 1.6, 4.0, and 8.0 kA/m (solid lines indicate decreasing stress from 60 MPa to −60 MPa, dashed lines indicate increasing stress from −60 MPa to 60 MPa).

the dashed line curve exhibits a higher peak sensitivity than the solid line. The opposite is true for 4.0 and 8.0 kA/m. This reversal and the associated hysteresis are due to the magnetomechanical nonlinearity and hysteresis of Galfenol.

B. Minor magnetization loops under constant field

Fig. 5(a) shows minor magnetization loops obtained from a 4.0 Hz, 2.8 MPa amplitude sinusoidal stress superimposed on dc compressive stresses ranging from −40.7 MPa to −5.6 MPa at 7.0 MPa intervals and bias magnetic fields ranging from 1.6 kA/m to 8.0 kA/m in 0.8 kA/m steps. The bias magnetic fields were applied in constant field mode. Distinct magnetization regions are observed depending on stress and field values. For example, when the dc compressive stress is −5.6 MPa, a bias field of 1.6 kA/m produces the largest magnetization range. When the dc compressive stress is −26.6 MPa, magnetization changes the most at a bias magnetic field of 5.6 kA/m. Overlaying major magnetization versus stress loops from Fig. 2(a) with minor loops from Fig. 5(a) for 1.6, 4.0, and 8.0 kA/m magnetic fields provides a comparison of magnetization responses as shown in Fig. 5(b). The effect of the minor loop cyclic stress is to settle the magnetomechanical state of the sample without going to stress extremes of the major stress loop. In Fig. 5(b), the minor loops fall within the major loops. A feature of Fig. 5(b) is that the average slope of the minor magnetization loops is consistently flatter than their enclosing major magnetization loop.

It is emphasized that the minor loop tests were conducted at 4.0 Hz for consistency with similar work on Terfenol-D presented in the literature.[20] Our measurements show that testing at 0.04 Hz or 4 Hz does not change the difference in slope between the minor and the major loops. At a prestress of −14 MPa and field of 1.6 kA/m, for example, the difference between 0.04 Hz and 4 Hz measurements is 2.92 kA/m/MPa which is equivalent to 3.66 T/GPa. In contrast, the sensitivity difference between minor and major loops is about 22 T/GPa (Fig. 5(c)). The flatter slope is thus attributed to the intrinsic differences between minor and major loops, which is consistent with Terfenol-D measurements.[20]

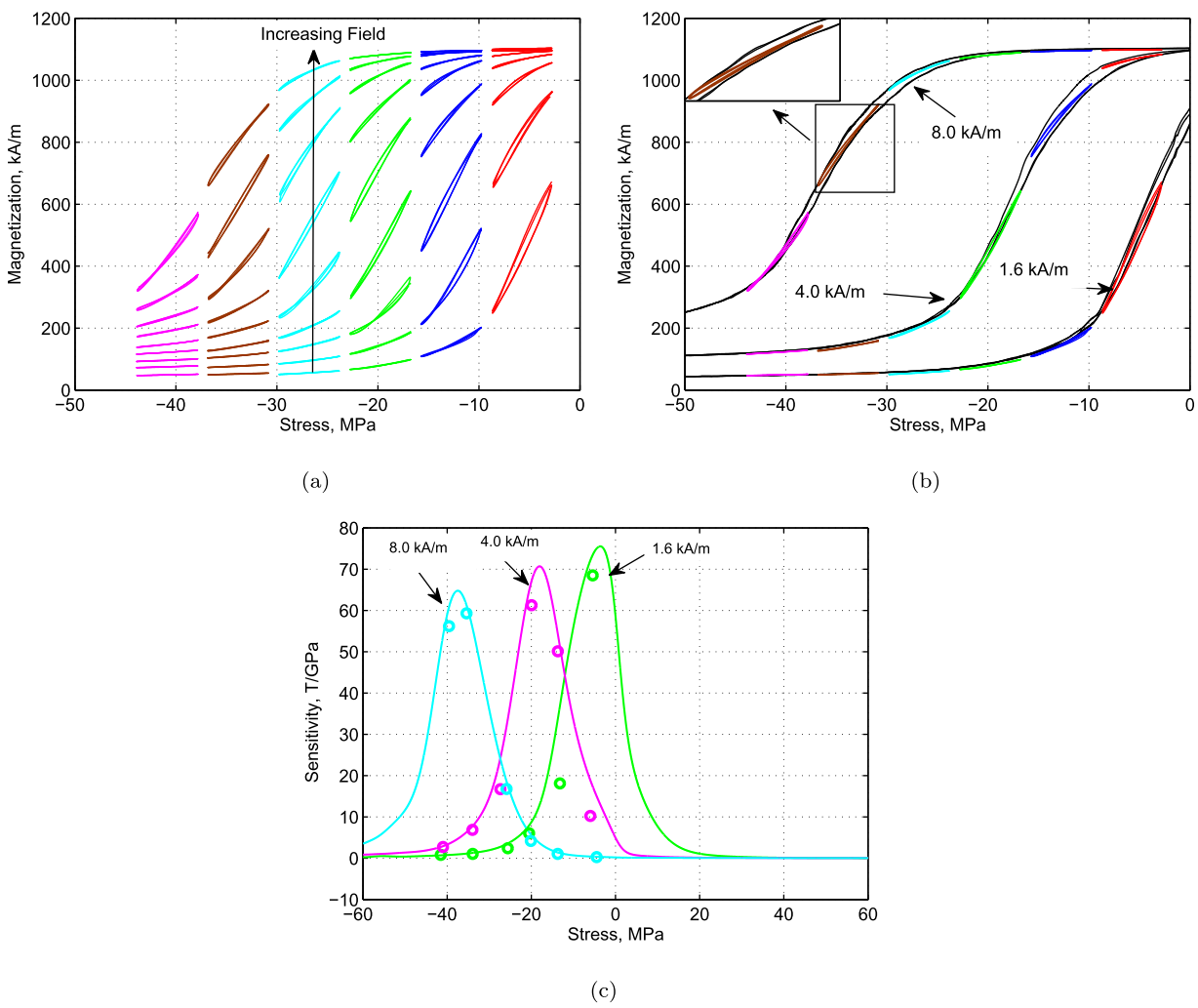

FIG. 5. (a) Minor magnetization loops with a 4.0 Hz, 2.8 MPa cyclic stress superimposed on different dc compressive stresses ranging from −40.7 MPa to −5.6 MPa in 7.0 MPa steps and bias fields ranging from 1.6 kA/m to 8.0 kA/m at 0.8 kA/m intervals. (b) Major and minor magnetization loops for bias fields 1.6, 4.0, and 8.0 kA/m. (c) Sensitivity from major and minor magnetization loops for bias fields of 1.6, 4.0, and 8.0 kA/m (solid lines show sensitivity from major loops; circle markers denote sensitivity from minor loops).

Sensitivity versus stress curves calculated from major and minor magnetization loops at bias fields of 1.6, 4.0, and 8.0 kA/m are shown in Fig. 5(c). Sensitivity from major loops is indicated with solid lines, whereas the circle markers show sensitivity calculations from minor loops. The latter was obtained through a least squares regression fit on each minor loop in Fig. 5(a). In Fig. 5(c), the sensitivity from minor loops is consistently lower than from major loops. For example, when the magnetic field is 4.0 kA/m, the sensitivity is about 67 T/GPa from the major loop while it is about 62 T/GPa from the minor loop at the same applied stress (−20 MPa).

C. Major magnetization loops under constant current

Practical devices such as force sensors or energy harvesters will typically lack active magnetic field control. In constant-current mode, the magnetic field does not exactly track the current due to the nonlinear relationship between circuit reluctance and field, and between field and current. The magnetization in either field or current control is different as a result.[5,6,17] Major and minor magnetization versus stress loops were measured to quantify this difference.

Magnetization as a function of stress under different constant currents is shown in Fig. 6(a). The measured relationship between magnetic field and stress at various constant currents is shown in Fig. 6(b); for a given constant current, the magnetic field does vary as stresses are applied. One feature of the Evans and Dapino energy-averaged model is that it quantifies input-output system relations, i.e., it can take currents (or voltages) as input rather than magnetic fields. Fig. 6(c) shows both experimental measurements and energy-averaged model calculations. The model error is small overall (1.38%). However, at low constant current (98 mA and 204 mA) and low tensile stresses, the model exhibits overshoot-type behavior that is only partially present in the data (refer to the 204 mA curve). The overshoot is due to the opposite effects of tension application: on the one hand, increasing tension increases magnetization; on the other hand, increasing tension decreases magnetization through a decrease in the magnetic field. These effects are not observed when the field is taken as model input. At high bias currents, the alloy is almost saturated which means that the magnetic energy is dominant, and stress-induced magnetic field variations result in small changes in magnetization; therefore, no magnetization overshoot is present.

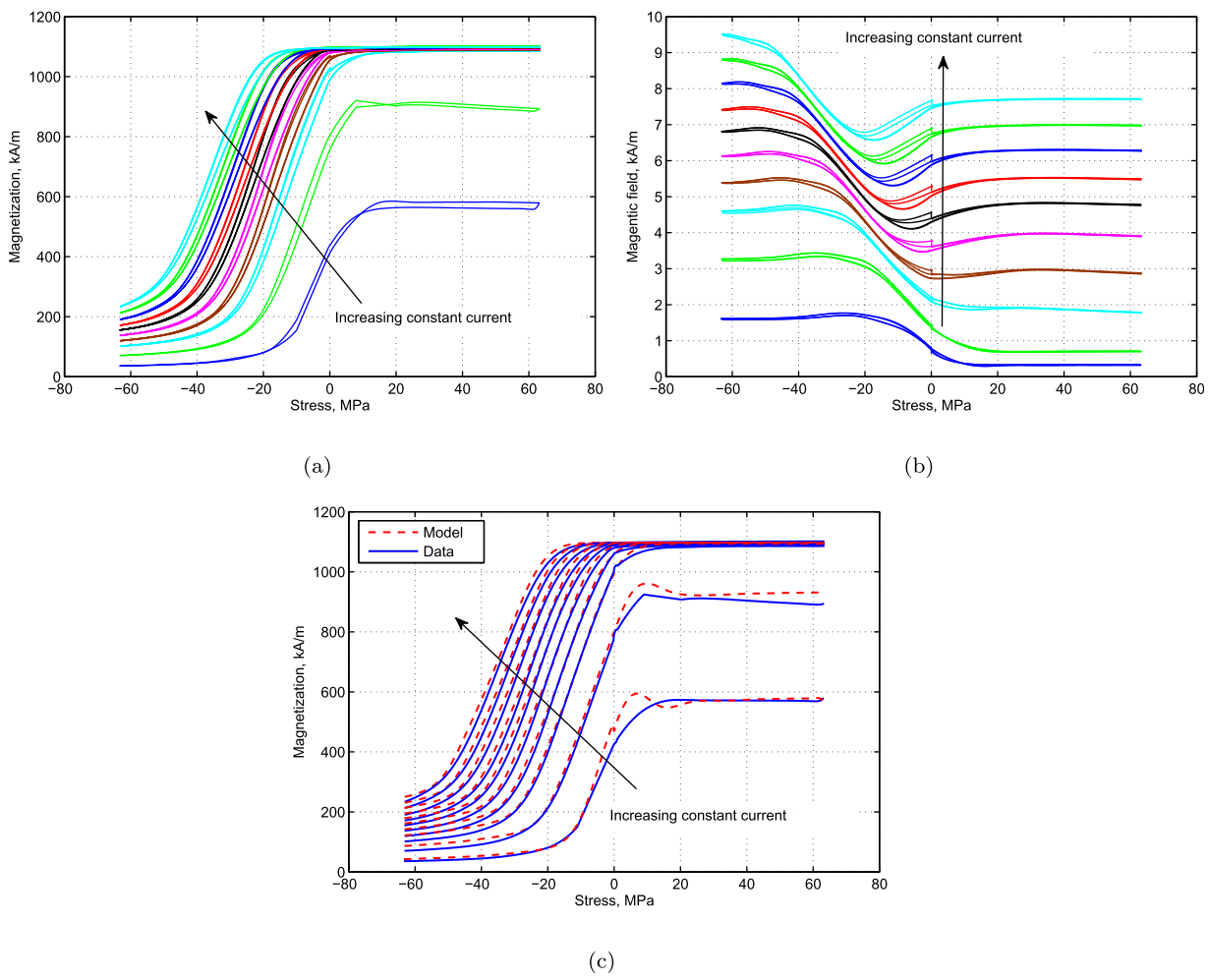

FIG. 6. (a) Magnetization versus stress for different constant currents: 98, 204, 288, 338, 384, 426, 464, 508, 550, and 596 mA. (b) Magnetic field versus stress for the same bias currents. (c) Calculated and measured anhysteretic magnetization under constant-current biasing.

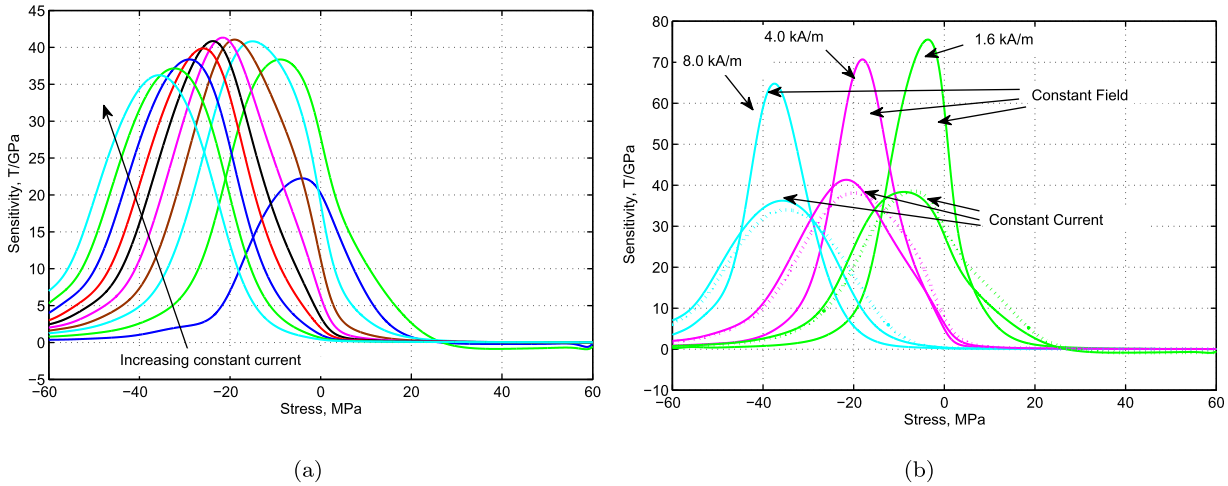

FIG. 7. (a) Sensitivity versus stress for constant current measurements (stresses decreased from 60 MPa to −60 MPa). (b) Sensitivity versus stress for constant field and constant current at comparable bias magnetic fields of 1.6, 4.0, and 8.0 kA/m. The solid lines indicate decreasing stress from 60 MPa to −60 MPa while the dashed lines indicate increasing stress from −60 MPa to 60 MPa.

The model parameters used in Fig. 6(c) are the same as for constant field: $K = 27.1\,\mathrm{kJ/m^3}$, $K_0 = 0.021\,\mathrm{kJ/m^3}$, $\mu_0 M_s = 1.3787\,\mathrm{T}$, $\lambda_{100} = 156.56 \times 10^{-6}$, and $\Omega = 776.73\,\mathrm{J/m^3}$.

Comparison of constant field and constant current major loops, Figs. 2(a) and 6(a), respectively, shows that the latter has a flatter slope in the burst or high sensitivity region. In current control mode, increased compression leads to a magnetic field increase over that achieved at constant field (Fig. 6(b)), thus leading to greater magnetization at the same stress. At −40 MPa, for instance, the magnetization at field-controlled 7.2 kA/m is about 300 kA/m, whereas at the same stress, the magnetization is close to 550 kA/m at current-controlled 596 mA. These are comparable conditions as the field created by 596 mA is 7.5 kA/m at zero load (see Fig. 6(b)).

Saturation occurs at about the same stress point in either case so long as the field is higher than 0.8 kA/m or the current is higher than 288 mA. A bias field of 0.8 kA/m is not sufficient to align the domains along the field direction; a tensile stress helps to achieve partial alignment and a magnetization change from 380 kA/m to 980 kA/m in Fig. 2(a). However, the magnetization changes from 420 kA/m to 570 kA/m in Fig. 6(a) when tensile stress is applied under constant current. Hysteresis in this case is more significant than it is in the data for constant field.

The sensitivity versus stress at constant current in Fig. 7(a) was calculated from data in which the stress was decreased from tension to compression using the same method as in Fig. 4(a). The sensitivity at constant current is lower than at constant field. For example, the maximum sensitivity is about 41 T/GPa for 384 mA (nominal bias field of about 4.0 kA/m), while it is 71 T/GPa for the same constant field of 4.0 kA/m. At constant current, the magnetomotive force and consequently the magnetic field through the sample increases as Galfenol's permeability goes down on application of compressive stresses. This increase in magnetic field decreases the drop in magnetization leading to lower sensitivity.[3]

Another significant feature is that the peak sensitivity first increases with increasing current and then decreases. Fig. 7(b) shows the sensitivity for comparable bias fields (1.6, 4.0, and 8.0 kA/m) under constant current and constant field, and also shows the sensitivity when stresses are both increasing and decreasing for constant current. The field controlled sensitivity is significantly higher, though the peaks are sharper indicating lower stress bandwidth. Under the same bias magnetic field, the sensitivity peak occurs at almost the same stress levels for constant current and constant field. The point at which the peak occurs is when the applied compressive stress balances the anisotropy energy and magnetic field energy. Hysteresis is observed in Fig. 7(b) when stress is increasing and decreasing, more so than at constant field (shown in Fig. 4(b)). The reason is that the permeability varies at constant current. From the viewpoint of energy loss, the constant field measurement shows less energy loss because the feedback control of field compensates parts of the loss.

D. Minor magnetization loops under constant current

Minor magnetization loops with a 4.0 Hz, 2.8 MPa amplitude sinusoid stress superimposed on different dc compressive stresses ranging from −40.7 MPa to −5.6 MPa in 7.0 MPa steps and different constant currents of 204, 288, 338, 384, 426, 464, 508, 550, and 596 mA are shown in Fig. 8(a). Overlaying the major magnetization versus stress loops of Fig. 6(a) with minor loops from Fig. 8(a) for the 1.6, 4.0, and 8.0 kA/m bias magnetic fields provides a comparison of magnetization responses as shown in Fig. 8(b). The minor loops fall within major magnetization loops. The average slope of the minor loops is consistently flatter than their enclosing major loop.

The sensitivity as a function of stress from both major and minor magnetization loops for constant current is shown in Fig. 8(c), where solid lines represent sensitivity from major loops and the circle markers are the sensitivity from minor loops. These discrete points were calculated from a least squares regression fit on each minor loop in Fig. 8(a). As before, the sensitivity from minor loops is lower than that from major loops.

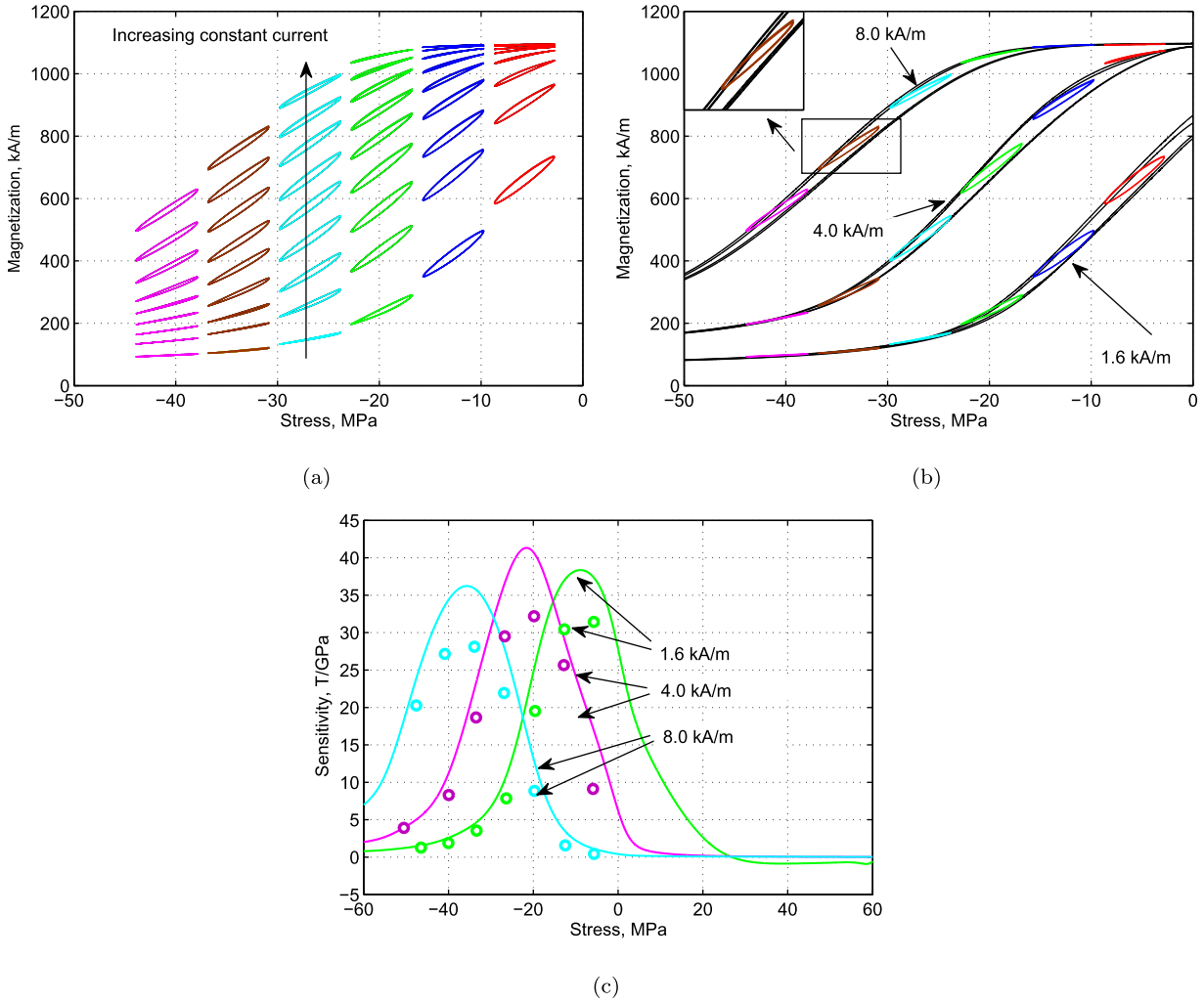

FIG. 8. (a) Minor magnetization loops under a 4.0 Hz, 2.8 MPa cyclic stress superimposed on different dc compressive stresses ranging from −40.7 MPa to −5.6 MPa in 7.0 MPa steps and constant current of 204, 288, 338, 384, 426, 464, 508, 550, and 596 mA. (b) Major and minor magnetization loops for bias fields of 1.6, 4.0, and 8.0 kA/m. (c) Sensitivity from major and minor magnetization loops for bias fields of 1.6, 4.0, and 8.0 kA/m (solid lines are sensitivity from major loops, circle markers are sensitivity from minor loops).

V. CONCLUDING REMARKS

In this work, major magnetization and stress loops with different bias magnetic fields from 0.8 kA/m to 8.0 kA/m in 0.8 kA/m steps were measured in research-grade, ⟨100⟩ oriented, textured polycrystalline $Fe_{81.6}Ga_{18.4}$. Compressive and tensile stresses were applied from −63 MPa to 63 MPa, whereas bias magnetic fields were applied with both a constant current and a constant field. The results show that both in constant current and in constant field, when the bias field is larger than 2.4 kA/m, application of tensile stress does not significantly alter the magnetization because at those fields the domains have aligned along the ⟨100⟩ direction. When the bias field is 0.8 kA/m or 1.6 kA/m, however, the magnetization changes considerably with tensile stress. The amount of hysteresis is reduced in the constant field measurements. The Evans and Dapino energy-averaged model was implemented and compared against experimental measurements both under constant field and constant current. The results show that there is close agreement with an error of 1.18% for constant field results and 1.38% for constant current results.

Minor loops were generated by superimposing a 4.0 Hz, 2.8 MPa amplitude sinusoidal stress on different dc compressive stresses ranging from −40.7 MPa to −5.6 MPa in 7.0 MPa steps. The slope of magnetic flux density versus stress, that is, the sensitivity for stress was calculated. The sensitivity from major loops was calculated from data in which the stress was decreasing from tension to compression. The peak sensitivity moves progressively towards increasing compressive stress as the bias field increases. Results show that the peak sensitivity in constant field is greater than that under constant current; the sensitivity in constant current is flatter than that at constant field. The sensitivity from minor loops was plotted with discrete plots calculated from a least squares regression fit on each minor loop. The sensitivity for minor loops is consistently lower than for major loops, whether at constant field or constant current.

ACKNOWLEDGMENTS

We wish to acknowledge the financial support from the following sources: Office of Naval Research MURI Grant

N000140610530; the member organizations of the Smart Vehicle Concept Center (www.SmartVehicleCenter.org), a National Science Foundation Industry/University Cooperative Research Center (I/UCRC); National Natural Science Foundation of China (Grants Nos. 50971056, 51171057, 51201055); and Natural Science Foundation of Hebei Province (Grant No. E2011202002).

[1]J. Atulasimha and A. B. Flatau, Smart Mater. Struct. **20**, 043001 (2011).
[2]M. J. Dapino, Struct. Eng. Mech. **17**, 303 (2004).
[3]J. Atulasimha, A. B. Flatau, and R. A. Kellogg, J. Intell. Mater. Syst. Struct. **17**, 97 (2006).
[4]J. Atulasimha and A. B. Flatau, J. Intell, Mater. Syst. Struct. **19**, 1371 (2008).
[5]J. Atulasimha, A. B. Flatau, and J. R. Cullen, Smart Mater. Struct. **17**, 025027 (2008).
[6]J. Atulasimha, A. B. Flatau, and J. R. Cullen, J. Appl. Phys. **103**, 014901 (2008).
[7]S. Datta, J. Atulasimha, C. Mudivarthi, and A. B. Flatau, J. Magn. Magn. Mater. **321**, 4017 (2009).
[8]S. Datta, J. Atulasimha, C. Mudivarthi, and A. B. Flatau, J. Magn. Magn. Mater. **322**, 2135 (2010).
[9]P. G. Evans and M. J. Dapino, J. Appl. Phys. **107**, 063906 (2010).
[10]P. G. Evans and M. J. Dapino, IEEE Trans. Magn. **44**, 1711 (2008).
[11]P. G. Evans and M. J. Dapino, J. Appl. Phys. **105**, 113901 (2009).
[12]P. Weetman and G. Akhras, Appl. Phys. Lett. **95**, 072504 (2009).
[13]J. Atulasimha, A. B. Flatau, and E. Summers, Smart Mater. Struct. **16**, 1265 (2007).
[14]A. Mahadevan, P. G. Evans, and M. J. Dapino, Appl. Phys. Lett. **96**, 012502 (2010).
[15]P. G. Evans and M. J. Dapino, J. Appl. Phys. **108**, 074517 (2010).
[16]J. B. Restorff, M. Wun-Fogle, and E. Summers, J. Appl. Phys. **109**, 07A922 (2011).
[17]A. Mahadevan, M.S. thesis, The Ohio State University, Columbus, OH, 2009.
[18]S. Chakrabarti and M. J. Dapino, Smart Mater. Struct. **20**, 105034 (2011).
[19]W. D. Armstrong, J. Appl. Phys. **81**, 2321 (1997).
[20]R. Kellogg and A. Flatau, J. Intell. Mater. Syst. Struct. **19**, 583–595 (2008).